

Normal and Feature Approximations from Noisy Point Clouds *

Tamal K. Dey Jian Sun †

Abstract

We consider the problem of approximating normal and feature sizes of a surface from point cloud data that may be noisy. These problems are central to many applications dealing with point cloud data. In the noise-free case, the normals and feature sizes can be approximated by the centers of a set of unique large Delaunay balls called *polar* balls. In presence of noise, polar balls do not necessarily remain large and hence their centers may not be good for normal and feature size approximations. Earlier works suggest that some large Delaunay balls can play the role of polar balls. However, these results were short in explaining how the big Delaunay balls should be chosen for reliable approximations and how the approximation error depends on various factors. We provide new analyses that fill these gaps. In particular, they lead to new algorithms for practical and reliable normal and feature approximations.

1. Introduction

Recently, a number of algorithms have been designed for processing point cloud data. Often these algorithms, as a basic step, estimate the normals and features of the sampled surface from the given point cloud. For example, some algorithms [1, 8, 11] need a normal estimation step for surface reconstruction, and others estimate the scale of local geometry also called the local feature size to handle non-uniform samples [9, 14]. In the noise-free case the problem of normal and feature size approximations have been well studied [2, 4, 6]. In the case of noise, optimization based techniques [1, 13] are known for normal approximations though they do not have theoretical guarantees. It is known that results from the noise-free case can be extended by using big Delaunay balls that can help in estimating normals [8] with theoretical guarantees. However, it is not known how the error of approximation depends on different noise components, and more importantly, how the big Delaunay balls should be chosen for reliable approximations. The problem for feature approximations in

presence of noise is much less understood. No reliable and practical algorithm is known for it. In this paper we address these open issues.

Motivation and results. Amenta and Bern [2] introduced the concept of poles. These are the furthest Voronoi vertices from the respective sites on the two sides of the sampled surface. In terms of the Delaunay triangulation, poles are the centers of the largest Delaunay balls incident to the sample points on both sides of the sampled surface. These balls are also called the polar balls. Amenta and Bern showed that, in the noise-free case, the normals can be estimated by the poles. Further, Amenta, Choi, Kolluri [4] and Boissonnat, Cazals [6] proved that the poles also approximate the medial axis and hence local feature sizes can be estimated by distances to the poles.

In the presence of noise, the above results do not hold since some of the polar balls can be arbitrarily small with their centers being arbitrarily close to the surface. See the top-middle picture in Figure 1. Nevertheless, Dey and Goswami [8] observed that, under a reasonable noise model, many Delaunay balls remain big and their centers can help in approximating the normals. The error in the normal approximation by big Delaunay balls obviously depends on the sampling density (ε) and also on the size of the chosen Delaunay balls. A detailed analysis on these dependencies is missing in earlier works. First, our analysis provides an error bound that unifies earlier results. Second, it tells us how to choose big Delaunay balls in practice for reliable normal and, in particular, feature size approximations for noisy point clouds.

In the noise-free case the choice of the Delaunay balls is not an issue in normal and feature size approximations as they are approximated from polar balls which are almost as big as medial balls. However, in the case of noise, the choice of Delaunay balls is an issue as all polar balls are not big. To remain scale independent one can choose Delaunay balls whose radii are larger than a threshold determined by some nearest neighbor distances of the sample points incident on the Delaunay balls. In order to gauge the viable values of the threshold, it is important to know how the normal and feature size approximation errors depend on the radii of the Delaunay balls. Our new analysis provides this relation. We show that normals can be estimated from Delaunay

*This work is partially supported by NSF CARGO grant DMS-0310642 and ARO grant DAAD19-02-1-0347.

†Department of Computer Science and Engineering, The Ohio State U., Columbus, OH 43210, USA.

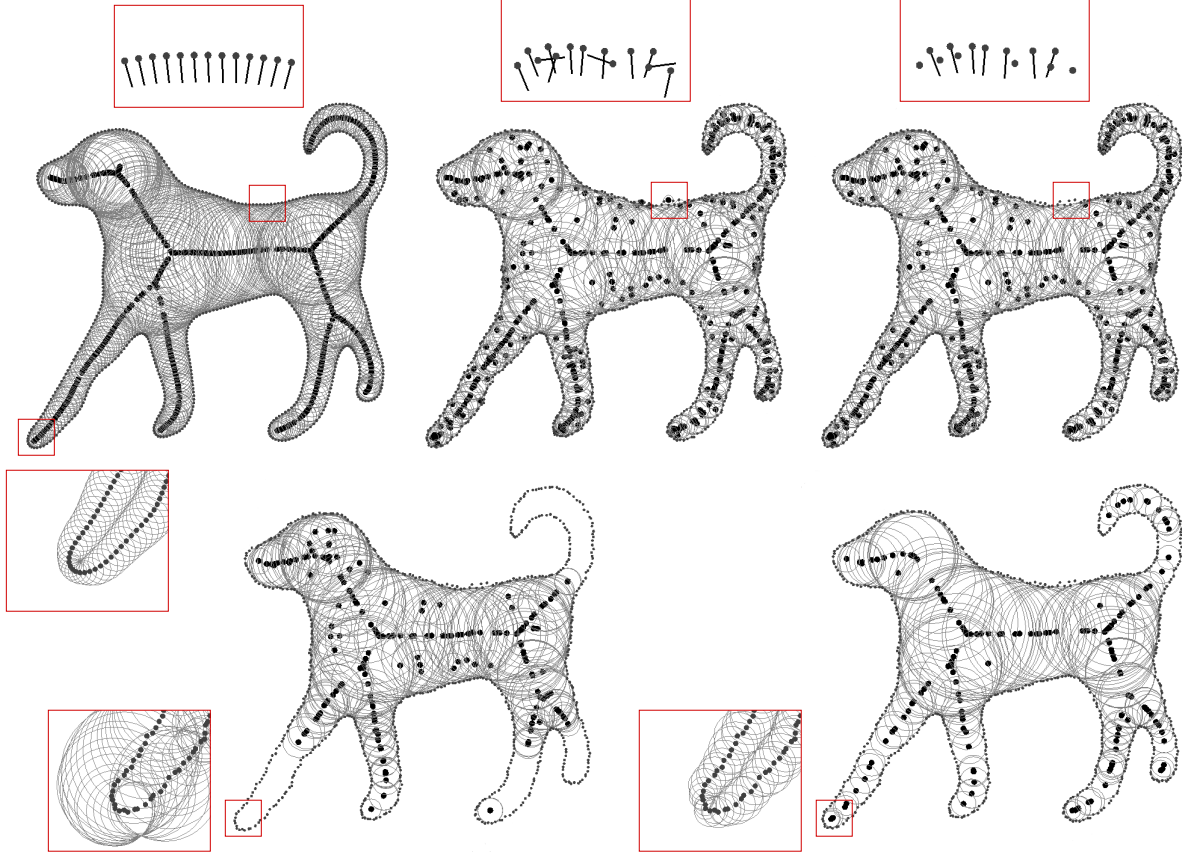


Figure 1: Top row: Left: noise-free case, poles are approximating the medial axis and normals well. Middle: A small noise disturbs the poles significantly resulting in poor normal and medial axis approximation with all poles. Right: only a subset of big Delaunay balls are chosen, normals though not medial axis are well approximated. Bottom row: Left: Delaunay balls of bigger size are chosen to exclude unwanted poles, some significant parts of the medial axis are not approximated. Right: Centers of polar balls chosen with our algorithm approximate the medial axis everywhere. Approximated feature sizes are indicated in the highlighted boxes.

balls that are not necessarily as big as local feature sizes ($f(\cdot)$). In fact, Delaunay balls with radii as small as $\varepsilon^{\frac{1}{2}} f(\cdot)$ are also good for normal estimations. See top row in Figure 1 for an illustration.

The case for feature estimations in presence of noise is far more difficult. This is because, unlike normal approximations, not all centers of Delaunay balls chosen with a reasonable threshold approximate the medial axis. Choosing the right ones is hard. If the threshold is relatively small, a number of centers remain which do not approximate the medial axis. See top-right picture in Figure 1. On the other hand if the threshold is large, the medial axis for some parts of the models may not be approximated at all; see bottom-left picture in Figure 1. As a result no threshold may exist for which large Delaunay balls' centers approximate the medial axis, the DOG data in Figure 1 and the HORSE data in Figure 8 are two such

examples in two and three dimensions respectively.

We propose a different algorithm to choose the Delaunay balls for approximating the medial axis. We consider k -nearest neighbors for some k and take the largest polar ball's center among these neighbors to approximate the medial axis. Our analysis leads to this algorithm which frees us from the burden of choosing a size threshold. Our experiments suggest that k can be chosen fairly easily, generally in the range of 5 to 10. The most important thing is that a k can be found for which the medial axis is well approximated where no such size threshold may exist. The bottom row of Figure 1 illustrates this point.

Previous results. Amenta, Bern and Eppstein [3] introduced the ε -sampling for noise-free case. This requires each point on the surface to have a sample point within a distance of ε times the local feature size.

When noise is allowed, the sample points need not lie exactly on the surface and may scatter around it. Therefore, the sampling model needs to specify both a *tangential scatter*, i.e., the sparseness of the sampling along tangent directions of the surface and also a *normal scatter*, i.e., the sparseness of sampling along the normal directions. Dey and Goswami [8] introduced a noise model that uses the same sampling parameter ε for both scatters. Kolluri [11] and later Dey and Sun [9] modified the normal scatter to have ε^2 dependence. The errors of normal and feature approximations depend on both tangential and normal scatters. Therefore, we introduce two independent parameters ε and δ for these two scatters to reveal the dependence of the approximation errors on these two parameters separately.

Normal approximation: Dey and Goswami [8] and Mederos et al. [12] showed that when both tangential and normal scatters are $O(\varepsilon)$ times the local feature size, the normals can be approximated with an $O(\sqrt{\varepsilon})$ error if the chosen Delaunay balls have radius almost as big as the local feature size. Dey and Sun [9] showed that the error is $O(\varepsilon)$ if the normal scatter is only $O(\varepsilon^2)$ times the local feature size. None of these results specify how the error depends on the radii of the chosen Delaunay balls.

In this paper we provide a simple elegant analysis which shows that the error is $2(\frac{1}{\lambda} + 1)O(\varepsilon + \sqrt{\delta})$ where λ is the radius of the Delaunay ball. Previous results under different noise models can be derived from this unified result. One implication of this result is that Delaunay balls as small as $O(\varepsilon^{\frac{1}{2}} + \delta^{\frac{1}{4}})f(\cdot)$ can help in estimating the normals. This relaxes the burden on setting the parameter for the normal estimation algorithm.

Feature approximation: Amenta, Bern and Eppstein [3] defined the local feature size of a point x on the surface as the distance of x to the medial axis. Obviously, the local feature size can be estimated if the medial axis can be approximated. An algorithm for approximating the medial axis from noisy point clouds exists [7]. This algorithm approximates the medial axis with Voronoi faces under a stringent uniform sampling condition. Selecting Voronoi faces to approximate the medial axis is not a simple task in practice even for noise-free case [5, 10] and it is not clear how this algorithm works in practice when noise is present. Moreover, for estimating the local feature size a continuous approximation with Voronoi faces is an overkill. A discrete approximation of the medial axis with a set of Voronoi vertices serves the purpose equally well. For the noise-free case, such an approximation was proposed by Amenta et al. [4] and Boissonnat and Cazals [6]. Re-

cently, Mederos et al. [12] derived some results for noisy point clouds that have some connections to the local feature size approximations though the approximation factor depends on a surface related constant which can be potentially huge.

Our analysis is free of any surface dependent constant and it relates the approximation error to the tangential and normal scatters separately. Most importantly, the analysis justifies our choice of polar balls based on nearest neighbors to approximate the medial axis. Figure 1 and 8 show that this choice is far more superior than the big Delaunay ball strategy. Experiments with our implementation [15] of the algorithm confirm this claim for other models.

2. Preliminaries

2.1 Definitions

For a set $Y \subseteq \mathbb{R}^3$ and a point $x \in \mathbb{R}^3$, let $d(x, Y)$ denote the Euclidean distance of x from Y ; that is,

$$d(x, Y) = \inf_{y \in Y} \{\|y - x\|\}.$$

The set $B_{c,r} = \{y \mid y \in \mathbb{R}^3, \|y - c\| \leq r\}$ is a *ball* with radius r and center c .

Voronoi and Delaunay diagram. For a finite point set $P \subset \mathbb{R}^3$, we will denote the Voronoi diagram and its dual Delaunay triangulation of P by $\text{Vor } P$ and $\text{Del } P$ respectively. The Voronoi cell for a point p is denoted as V_p .

Sampled surface. Let $\Sigma \subset \mathbb{R}^3$ be a compact smooth surface without boundary from which the input sample is derived possibly with noise. Also, assume that Σ is connected. The bounded and unbounded components of $\mathbb{R}^3 \setminus \Sigma$ are denoted Ω_I and Ω_O respectively. The normal at any point $x \in \Sigma$ is denoted \mathbf{n}_x which is directed locally inward, i.e., toward Ω_I .

The *medial axis* M of Σ is the locus of the centers of the maximal balls whose interiors are empty of points in Σ . These balls meet Σ only tangentially. We call each such ball $B_{m,r}$ a *medial ball* where $r = d(m, \Sigma)$. Barring some pathological cases, we can assume $M \cap \Sigma$ is empty if Σ is smooth. The subsets of M in Ω_I and Ω_O are called *inner* and *outer* medial axis respectively. For each point $x \in \Sigma$, there are two *medial balls*, one centering a point in the inner medial axis and the other in the outer medial axis. The *local feature size* at a point $x \in \Sigma$ is defined as $f(x) = d(x, M)$. The function $f(\cdot)$ satisfies the following Lipschitz property [2].

Lipschitz property. For any two points $x, y \in \Sigma$, $f(x) \leq f(y) + \|x - y\|$.

2.2 Sampling

A finite set of points $P \subset \Sigma$ is called an ε -sample of Σ if $d(x, P) \leq \varepsilon d(x, M)$ for each $x \in \Sigma$. To accommodate the tangential and normal scatters of points around Σ in the noisy case, we put two conditions on the sampling. The first condition says that the projection of the point set P on the surface makes a dense sample and the second one says that P is close to the surface. We also use a third condition to make the sampling locally uniform. To make the sampling definition general, we use a separate parameter for each sampling condition. For any point $x \in \mathbb{R}^3 \setminus M$ let \tilde{x} denote its closest point on Σ . Clearly, the segment $x\tilde{x}$ is parallel to the normal $\mathbf{n}_{\tilde{x}}$.

We say $P \subset \mathbb{R}^3$ is a $(\varepsilon, \delta, \kappa)$ -sample of Σ if the following conditions hold.

- (i) $\tilde{P} = \{\tilde{p}\}_{p \in P}$ is an ε -sample of Σ ,
- (ii) $\|p - \tilde{p}\| \leq \delta f(\tilde{p})$,
- (iii) $\|p - q\| \geq \varepsilon f(\tilde{p})$ for any two points p, q in P where q is the κ th nearest sample point to p .

Figure 2 illustrates why we put the third condition. In the figure the same point sample satisfies the first two conditions for two different curves; C and also $C \cup C'$. Our analyses for normal and medial axis approximations apply to both of these curves; albeit with different scales of local feature sizes. Therefore, the analyses do not need the third condition in the sampling. However, our approximation algorithms determine a particular scale by looking at the nearest neighbor distances. This implies that the sampling cannot allow the ambiguity which is forced by assuming a local uniformity constraint in the third one.



Figure 2: A point sample satisfying sampling conditions (i) and (ii) for a single component curve C (left) and also the curve $C \cup C'$ (right).

In the analysis we concentrate only in the bounded component Ω_I together with the inward normals and inner medial axis. It should be clear that the results also hold for unbounded component, outward normals and outer medial axis. For a point $x \in \Sigma$, let m_x denote the center of the inner medial ball meeting Σ at x and ρ_x its radius.

It follows almost immediately from our sampling conditions that each point of Σ and a point not far away from

Σ has a sample point nearby. Lemma 1 and Corollary 2 formalize this idea.

Lemma 1. *Any point $x \in \Sigma$ has a sample point within $\varepsilon_1 f(x)$ distance where $\varepsilon_1 = (\delta + \varepsilon + \delta\varepsilon)$.*

Proof. From the sampling condition (i), we must have a sample point p so that $\|x - \tilde{p}\| \leq \varepsilon f(x)$. Also, $\|p - \tilde{p}\| \leq \delta f(\tilde{p}) \leq \delta(1 + \varepsilon)f(x)$. Thus,

$$\begin{aligned} \|x - p\| &\leq \|x - \tilde{p}\| + \|\tilde{p} - p\| \\ &\leq \varepsilon f(x) + \delta(1 + \varepsilon)f(x) \\ &\leq (\delta + \varepsilon + \delta\varepsilon)f(x). \end{aligned}$$

□

Since $f(x) \leq \rho_x$ for any point $x \in \Sigma$, the following corollary is immediate.

Corollary 2. *Any point $y \in \mathbb{R}^3$ with $\|y - \tilde{y}\| = \delta\rho_{\tilde{y}}$ has a sample point within $\varepsilon_2\rho_{\tilde{y}}$ distance where $\varepsilon_2 = (2\delta + \varepsilon + \delta\varepsilon)$.*

3. Empty balls

A ball is *empty* if its interior is empty of points from P . A main ingredient in our analysis will be the existence of large empty balls. They in turn lead to the existence of large Delaunay balls that circumscribe Delaunay tetrahedra in $\text{Del } P$. The centers of such Delaunay balls which are also Voronoi vertices in $\text{Vor } P$ play crucial roles in the algorithms for normal and feature estimations. In this section, we present two lemmas that assure the existence of large empty balls with certain conditions.

Lemma 3 below assures that for each point $x \in \Sigma$ there is a large empty ball of radius almost as large as (i) $f(x)$ and (ii) ρ_x . Notice the differences between the distances of these balls from x . Also, see Figure 3.

Lemma 3. *A ball $B_{m,r}$ is empty of sample points from P if either*

- (i) $\tilde{m} = x$, $\|m - x\| = f(x)$ and $r = (1 - 3\delta)f(x)$,
or
- (ii) $m = m_x$ and $r = (1 - \delta)\rho_x$.

Proof. Let p be any point in P (the left picture of Figure 3). For (i) we have

$$\begin{aligned} f(\tilde{p}) \leq f(x) + \|x - \tilde{p}\| &\leq f(x) + \|x - m\| + \|m - \tilde{p}\| \\ &\leq 2f(x) + \|m - \tilde{p}\|. \end{aligned}$$

Then,

$$\begin{aligned} \|m - p\| &\geq \|m - \tilde{p}\| - \|p - \tilde{p}\| \geq \|m - \tilde{p}\| - \delta f(\tilde{p}) \\ &\geq \|m - \tilde{p}\| - \delta(2f(x) + \|m - \tilde{p}\|) \\ &= (1 - \delta)\|m - \tilde{p}\| - 2\delta f(x) \\ &\geq (1 - 3\delta)f(x) \end{aligned}$$

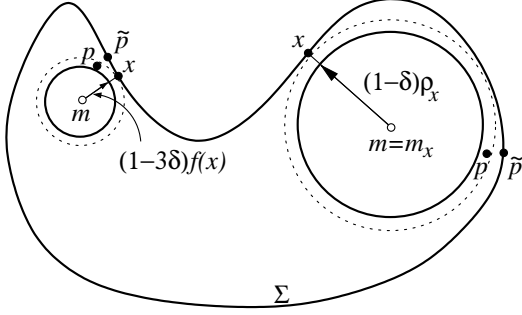


Figure 3: Illustration for Lemma 3. The dotted big balls are not empty of sample points but their slightly shrunk copies (shown with solid boundaries) are.

as $\|m - \tilde{p}\| \geq \|m - x\| = f(x)$. Therefore, p cannot be in the interior of B . Now consider (ii). We get

$$\begin{aligned} \|m_x - p\| &\geq \|m_x - \tilde{p}\| - \|p - \tilde{p}\| \\ &\geq \|m_x - \tilde{p}\| - \delta f(\tilde{p}) \\ &\geq \|m_x - \tilde{p}\| - \delta \|m_x - \tilde{p}\| \\ &= (1 - \delta) \|m_x - \tilde{p}\| \\ &\geq (1 - \delta) \rho_x \end{aligned}$$

as $\|m_x - \tilde{p}\| \geq \|m_x - x\| = \rho_x$.

□

Next, we show that, for each point x of Σ , there is a nearby large ball which is not only empty but also its boundary passes through a sample point close to x . Eventually these balls will be deformed to Delaunay balls for medial axis approximations.

Lemma 4. *For each point $x \in \Sigma$ there is an empty ball $B_{c,r}$ with $c \in \Omega_I$ that enjoys the following properties:*

- (i) r is at least $(1 - 2\sqrt{\varepsilon_2})\rho_x$, m_x is in $B_{c,r}$ and $\|c - m_x\| \leq 2\sqrt{\varepsilon_2}\rho_x$ where ε_2 defined in Corollary 2 is $O(\varepsilon + \delta)$,
- (ii) its boundary contains a sample point p within a distance $\varepsilon_3\rho_x$ from x where $\varepsilon_3 = 2\varepsilon_2^{\frac{1}{4}} + \delta$ and ε, δ are sufficiently small.

Proof. Consider the empty ball $B = B_{m_x, R}$ whose boundary passes through a point y where $\tilde{y} = x$ and $\|y - x\| = \delta\rho_x$ and $R = (1 - \delta)\rho_x$. Such a ball exists by Lemma 3 (ii) (see Figure 4).

SHRINKING: For a $\beta < 1$, let $B^\beta = B_{m_x, \beta R}$ be a further shrunk copy of B . The ball B and hence B^β are empty.

RIGID MOTION: Translate B^β rigidly by moving the center along the direction $\vec{m_x x}$ until its boundary hits a

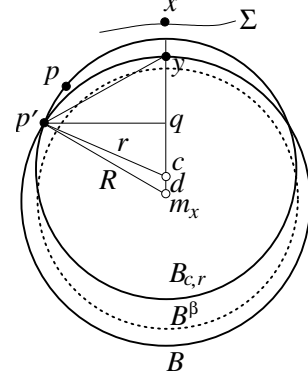


Figure 4: Illustration for Lemma 4.

sample point $p \in P$. Let this new ball be denoted $B_{c,r}$, refer to Figure 4.

Obviously $r = \beta R$. Let $d = \|c - m_x\|$. First we claim

$$(1 - \beta)R \leq d \leq (1 - \beta)R + \varepsilon_2\rho_x.$$

The first half of the inequality holds since B is empty of samples and hence B^β has to move out of it to hit a sample point. The second half of the inequality holds since from Corollary 2, a ball centered at y with radius $\varepsilon_2\rho_x$ cannot be empty of samples.

Next we obtain an upper bound on $\|y - p\|$. Refer to Figure 4. Since $\|p' - q\|^2 = \|c - p'\|^2 - \|c - q\|^2 = \|m_x - p'\|^2 - \|m_x - q\|^2$, we have

$$\|c - p'\|^2 - \|c - q\|^2 = R^2 - (\|c - q\| + d)^2$$

which gives

$$\|c - q\| = \frac{R^2 - r^2 - d^2}{2d}.$$

Hence

$$\begin{aligned} \|y - p\|^2 &\leq \|y - p'\|^2 \\ &= \|p' - q\|^2 + \|q - y\|^2 \\ &= R^2 - (d + \|c - q\|)^2 + (R - (d + \|c - q\|))^2 \\ &= 2R^2 - Rd - \frac{R}{d}(R^2 - r^2) \\ &\leq \frac{\varepsilon_2(1 + \beta)}{(1 - \delta)(1 - \beta) + \varepsilon_2} R^2. \end{aligned} \quad (3.1)$$

Since we want both $\|c - m_x\|$ and $\|x - p\|$ to be small, we take $\beta = 1 - \sqrt{\varepsilon_2}$. Then $r = \beta R \geq (1 - 2\sqrt{\varepsilon_2})\rho_x$. Also $\|c - m_x\| \leq ((1 - \delta)\sqrt{\varepsilon_2} + \varepsilon_2)\rho_x \leq 2\sqrt{\varepsilon_2}\rho_x$, which is small compared to r given ε and δ are sufficiently small. So m_x stays inside $B_{c,r}$. In addition, from inequality 3.1 we have

$$\|y - p\| \leq \sqrt{\left(\frac{2 - \sqrt{\varepsilon_2}}{1 - \delta + \sqrt{\varepsilon_2}}\right)^{\frac{1}{2}} \varepsilon_2^{\frac{1}{2}} R} \leq 2\varepsilon_2^{\frac{1}{4}} \rho_x.$$

The bound on $\|p - x\|$ follows as $\|x - y\| = \delta\rho_x$. □

Observation: If we choose β to be a suitable constant between 0 and 1, the above proof gives $\varepsilon_3 = O(\sqrt{\varepsilon_2}) = O(\sqrt{\varepsilon + \delta})$ though the radius of the empty ball becomes a constant fraction of ρ_x . Also, the entire proof remains valid when we replace ρ_x with $f(x)$.

4. Normal approximation

We will approximate the normals by the vectors from the sample points toward the centers of the Delaunay balls incident to them. First, we derive an upper bound on this normal approximation error in Theorem 1. Then, we describe a simple algorithm for approximating the normals whose justification is given by the theorem and Lemma 4.

4.1 Analysis

The idea is to measure how much one can tilt an empty ball anchored at a point p with its center in the direction of $\mathbf{n}_{\tilde{p}}$ while keeping it empty. The amount of tilt depends on how close the sample points are and also how big the ball is.

Theorem 1. *Let $p \in P$ be incident to an empty ball $B_{c,r}$ where $r = \lambda f(\tilde{p})$ and $c \in \Omega_I$. Then,*

$$\sin(\angle \vec{pc}, \mathbf{n}_{\tilde{p}}) \leq 2\left(\frac{1}{\lambda} + 1\right)(\varepsilon_1 + 2\sqrt{\delta}) + O(\delta) + O(\varepsilon^2)$$

for a sufficiently small $\varepsilon > 0$ and $\delta > 0$.

Proof. Let $B = B_{c,r}$. Assume that \vec{pc} makes an angle β with the normal $\mathbf{n}_{\tilde{p}}$. Let B_{in} and B_{out} be two balls with radius $f(\tilde{p})$ and tangentially meeting the surface at point \tilde{p} as Figure 5 shows. Let m be the center of B_{out} . We know the surface Σ is outside these two balls. By Lemma 3 the ball $B' = B(m, (1 - 3\delta)f(\tilde{p}))$, a shrunk ball of B_{out} , is also empty of samples. Therefore no sample point is inside the shaded area, see Figure 5.

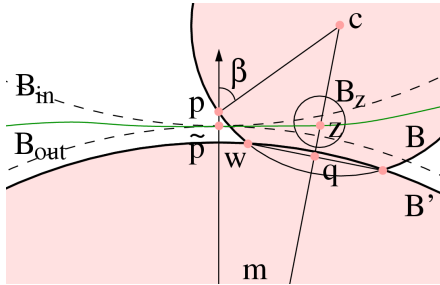


Figure 5: Illustration for Theorem 1.

Observation A. As β increases, the radius of the intersection circle of the boundaries of B and B' increases,

i.e. $\|w - q\|$ increases, and vice versa.

Observation B. Suppose that when $\|w - q\| = \sqrt{2}\varepsilon_1 f(\tilde{p})$ the angle β has the claimed bound. Then, if we show $\|w - q\| < \sqrt{2}\varepsilon_1 f(\tilde{p})$, we are done following Observation A.

Assume $\|w - q\| = \sqrt{2}\varepsilon_1 f(\tilde{p})$. Let z be the intersection point between Σ and the segment mc .

Consider the triangle formed by p , m and c . We have

$$(1 - \delta)f(\tilde{p}) \leq \|m - p\| \leq (1 + \delta)f(\tilde{p}),$$

$$\|c - p\| = \|c - w\| = \lambda f(\tilde{p})$$

and also $\|c - m\|$ equals

$$\sqrt{\|c - w\|^2 - \|w - q\|^2} + \sqrt{\|m - w\|^2 - \|w - q\|^2}.$$

If $\beta = \angle \vec{pc}, \mathbf{n}_{\tilde{p}}$,

$$\begin{aligned} \cos \beta &= \frac{\|c - m\|^2 - \|c - p\|^2 - \|m - p\|^2}{2\|c - p\|\|m - p\|} \\ &\geq \frac{(\sqrt{\lambda^2 - 2\varepsilon_1^2} + \sqrt{(1 - 3\delta)^2 - 2\varepsilon_1^2})^2 - \lambda^2 - (1 + \delta)^2}{2\lambda(1 + \delta)} \\ &\geq 1 - 2\left(1 + \frac{1}{\lambda}\right)^2(\varepsilon_1 + 2\sqrt{\delta})^2 + O(\delta^2) + O(\varepsilon_1^4). \end{aligned}$$

Hence

$$\begin{aligned} \sin \beta &\leq \sqrt{2(1 - \cos \beta)} \\ &\leq 2\left(1 + \frac{1}{\lambda}\right)(\varepsilon_1 + 2\sqrt{\delta}) + O(\delta) + O(\varepsilon_1^2). \end{aligned}$$

Now we show that $\|w - q\| < \sqrt{2}\varepsilon_1 f(\tilde{p})$ as required by Observation B.

Again, first assume that $\|w - q\| = \sqrt{2}\varepsilon_1 f(\tilde{p})$. We can show $\|\tilde{p} - z\| \leq 3\|\tilde{p} - m\| \tan \beta$. Therefore, from the bound on β $\|\tilde{p} - z\| = O(\varepsilon_1 + 2\sqrt{\delta})f(\tilde{p})$ which by Lipschitz property gives $f(z) < \sqrt{2}f(\tilde{p})$ given a sufficiently small δ and ε . We know $B_z = B(z, \varepsilon_1 f(z))$ with radius $\varepsilon_1 f(z) < \sqrt{2}\varepsilon_1 f(\tilde{p})$ has to contain at least one sample point by Lemma 1. This is impossible since B_z has a radius at most $\sqrt{2}\varepsilon_1 f(\tilde{p}) = \|w - q\|$ which means it lies completely in the shaded area. Therefore, $\|w - q\| \neq \sqrt{2}\varepsilon_1 f(\tilde{p})$. Now consider increasing $\|w - q\|$ beyond this distance while keeping z fixed. Notice that now z is not the intersection point between Σ and the segment mc . It is obvious that B_z remains inside the shaded area. Therefore, again we reach a contradiction to Lemma 1. Hence $\|w - q\|$ can not be larger than $\sqrt{2}\varepsilon_1 f(\tilde{p})$. \square

Implications: Theorem 1 gives a general form of the normal approximation under a fairly general sampling assumption. One can derive different normal approximation bounds under different sampling assumptions from this general result. For example, if P is a

$(\varepsilon, \varepsilon^2, -)$ -sample we get an $O(\varepsilon)$ bound on the normal approximation error. In case P is a $(\varepsilon, \varepsilon, -)$ -sample, we get an $O(\sqrt{\varepsilon})$ error bound. Another important implication is that Delaunay balls need not be too big to give good normal estimates. One can observe that if λ is only $\sqrt{\max\{\varepsilon, \delta\}}$, we get $O(\varepsilon^{\frac{1}{2}} + \delta^{\frac{1}{4}})$ error. Algorithmic implication of this fact is that a lot of sample points can qualify for normal estimation.

Observe that the proof of Theorem 1 remains valid even if the sample point p is replaced with any point $x \in \mathbb{R}^3$ meeting the conditions as stated in the corollary below. We use this fact later in feature estimation.

Corollary 5. *Let $x \in \mathbb{R}^3$ be any point with $\|x - \tilde{x}\| \leq \delta\rho_{\tilde{x}}$ and $B_{c,r}$ be any empty ball incident to x so that $r = \Omega(\rho_{\tilde{x}})$. Then, $\angle \tilde{x}c, \mathbf{n}_{\tilde{x}} = O(\varepsilon + \sqrt{\delta})$ for sufficiently small ε and δ .*

4.2 Algorithm

We know from Theorem 1 that if there is a big Delaunay ball incident to a sample point p , then the vector from p to the center of the ball estimates the normal direction at the point \tilde{p} . On the other hand, the observation after the proof of Lemma 4 assures that for each point $x \in \Sigma$, there is a sample point p within $O(\sqrt{\varepsilon + \delta})f(x)$ distance with an empty ball of radius $\Omega(f(x))$. This means there is a big Delaunay ball incident to p where the vector $p\tilde{c}$ approximates $\mathbf{n}_{\tilde{p}}$ and hence \mathbf{n}_x . Algorithmically we can exploit this fact by picking up sample points that are incident to big Delaunay balls only if we have a scale to measure ‘big’ Delaunay balls. For this we assume the third condition in the sampling which says that the sample is locally uniform.

Let λ_p be the distance of p to its κ th nearest neighbor. By sampling condition $\lambda_p \geq \varepsilon f(\tilde{p})$. Therefore, any Delaunay ball incident to p with radius more than $\tau\lambda_p$ will give a normal estimation with an error $6(\frac{1}{\tau\varepsilon} + 1)(\varepsilon)$ according to Theorem 1 under the assumption that P is a $(\varepsilon, \varepsilon^2, \kappa)$ -sample. It is important that λ_p is not arbitrarily large since then no Delaunay may qualify for the size threshold. This concern is alleviated by the fact that $\lambda_p \leq \varepsilon' f(\tilde{p})$ where $\varepsilon' = \left(\varepsilon + \frac{4\kappa + \varepsilon}{1 - 4\kappa\varepsilon}\right)\varepsilon$ [8].

Notice that the error decreases as τ increases. However, as we indicated before $\tau\varepsilon f(\tilde{p})$, the radius of the big Delaunay ball, can be as small as $\varepsilon^{\frac{1}{2}} f(\tilde{p})$ to give an $O(\sqrt{\varepsilon})$ error. This explains why a large number of Delaunay balls give good normal estimations as Figure 1 illustrates.

APPROXIMATENORMAL(P, τ)

 Compute Del P ;

 for each $p \in P$ compute λ_p ;

 if there is a Delaunay ball incident to p

with radius larger than $\tau\lambda_p$

 Compute the largest Delaunay ball $B_{c,r}$
 incident to p ;

 Approximate the normal direction at p by pc .

endif

Notice that, alternatively we could have eliminated the parameter τ in the algorithm by looking for the largest Delaunay ball incident to a set of k -nearest neighbors of p for some suitable k . Again, thanks to Lemma 4, we are assured that for a suitable k , one or more neighbors have Delaunay balls with radius almost equal to the medial balls. However, this approach limits the number of sample points where the normals are estimated. Because of our earlier observation, the normals can be estimated at more points where the Delaunay ball is big but not necessarily as big as the medial balls. In contrast, as we see next, feature estimation needs the Delaunay balls almost as big as the medial ones.

5. Feature approximation

We approximate the local feature size at a sample point p by first approximating the medial axis with a set of discrete points and then measuring the distance of p from this set. We are guaranteed by Lemma 4 that there are many sample points which are incident to big Delaunay balls. The furthest Voronoi vertices from these sample points in Ω_I and Ω_O approximate the inner and outer medial axis respectively. For a point $p \in P$, we call the furthest Voronoi vertex from p in $V_p \cap \Omega_I$ as the inner pole p^+ of p . Similarly one may define the outer pole p^- of p which resides in Ω_O .

In line with the previous results on medial axis approximation [4, 6, 7], we claim that a certain subset of the medial axis is approximated by poles. Let x and x' be two points where the medial ball B centered at m meets Σ . Call $\angle xm, x'$ the *medial angle* at m if it is the largest angle less than π made by any two such points of $B \cap \Sigma$. Let $M_\alpha \subseteq M$ be the subset where each point $m \in M_\alpha$ has a medial angle at least α .

5.1 Analysis

We show that each medial axis point m_x with a large enough medial angle is approximated by a pole. The idea is as follows. Consider the large ball incident to a sample point p guaranteed by Lemma 4. Then we deform it to a large Delaunay ball with the center at p^+ . First, during this deformation the ball cannot be tilted too much since the vector from p to the center has to approximate the normal $\mathbf{n}_{\tilde{p}}$ by Theorem 1. Second, the center in the tilted direction cannot move too much due to Lemma 6 as stated below. The result of these constraints is that the center p^+ of the Delaunay ball remains

close to the center of the original ball which in turn is close to m_x .

Lemma 6. *Let $B = B_{c,r}$ be an empty ball whose boundary passes through a sample point p . Let z be a point on Σ whose distance to the boundary of B is less than $\varepsilon' \rho_z$ for $\varepsilon' < 1$. Let $B' = B_{c',r'}$ be an empty ball obtained by expanding B while keeping c' on the ray \vec{pc} and p on its boundary. If $\beta \rho_z \leq r \leq \rho_z$, then we have*

$$\|c - c'\| \leq \frac{(\varepsilon_1 + \varepsilon')(2 + \varepsilon')}{2\beta(1 - \cos \angle pcz) - 2\varepsilon_1 - 2\varepsilon' \cos \angle pcz} \rho_z.$$

Proof. Let y be the closest point to z on the boundary of B . Obviously y, c and z are collinear. See Figure 6. We have $\|y - z\| \leq \varepsilon' \rho_z$. Let z' be the point where the line of $c'z$ intersects the boundary of B' . Since a ball centered at z with radius $\varepsilon_1 f(z)$ can not be empty of sample points by Lemma 1, we have $\|z' - z\| \leq \varepsilon_1 f(z) \leq \varepsilon_1 \rho_z$.

Consider the triangle made by c, c' and z . For convenience set $\angle pcz = \alpha$, $\|c - c'\| = \Delta c$, $\|z - z'\| = \Delta z$ and $\|y - z\| = \Delta y$. We know

$$\|c' - z\| = (\Delta c)^2 + \|c - z\|^2 + 2\Delta c \|c - z\| \cos \alpha.$$

This gives

$$(r + \Delta c - \Delta z)^2 = (\Delta c)^2 + (r + \Delta y)^2 + 2\Delta c (r + \Delta y) \cos \alpha$$

from which we get

$$\begin{aligned} \Delta c &= \frac{(r + \Delta y)^2 - (r - \Delta z)^2}{2(r - \Delta z) - 2(r + \Delta y) \cos \alpha} \\ &\leq \frac{(\varepsilon_1 + \varepsilon')(2 + \varepsilon')}{2\beta(1 - \cos \alpha) - 2\varepsilon_1 - 2\varepsilon' \cos \alpha} \rho_z. \end{aligned}$$

by plugging in $\Delta z \leq \varepsilon_1 \rho_z$, $\Delta y \leq \varepsilon' \rho_z$ and $\beta \rho_z \leq r \leq \rho_z$. \square

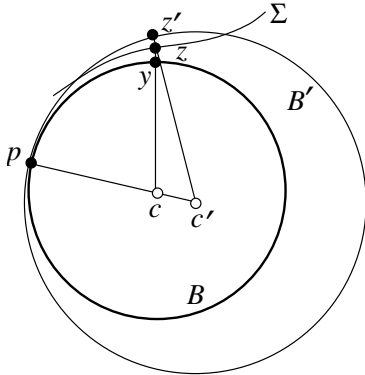


Figure 6: Illustration for Lemma 6.

Theorem 2. *For each point $m_x \in M_\alpha \cap \Omega_I$ where $\alpha = \varepsilon^{\frac{1}{4}} + \delta^{\frac{1}{4}}$, there is a sample point p within $O(\varepsilon^{\frac{1}{4}} + \delta^{\frac{1}{4}}) \rho_x$ distance of x so that the pole p^+ lies within $O(\varepsilon^{\frac{1}{4}} + \delta^{\frac{1}{4}}) \rho_x$ distance from m_x where ε and δ are sufficiently small.*

Proof. Consider the ball $B = B_{c,r}$ guaranteed by Lemma 4 whose boundary passes through a sample point p . Its radius r is $(1 - 2\sqrt{\varepsilon_2}) \rho_x$, $\|p - x\| \leq \varepsilon_3 \rho_x$ and $\|c - m_x\| \leq 2\sqrt{\varepsilon_2} \rho_x$. Let $B' = B_{p^+,r'}$ where p^+ is the inner pole of p and $r' = \|p - p^+\|$. The ball B' is Delaunay and its radius $r' \geq r \geq (1 - 2\sqrt{\varepsilon_2}) \rho_x$.

Focus on the two balls B and B' passing through p , see Figure 7. The ball B has m_x inside it which means that its radius is at least $(1 - \delta) f(\tilde{p})/2$. So, the radius of B' being bigger than that of B is also at least $(1 - \delta) f(\tilde{p})/2$. Therefore, by Theorem 1 the vectors \vec{pc} and \vec{pp}^+ make $O(\varepsilon + \sqrt{\delta})$ angle with $\mathbf{n}_{\tilde{p}}$ and at most double of this angle among them. Let c' be the point on the segment pp^+ so that pc' has the same length as pc . Clearly,

$$\|c - c'\| \leq \|p - c\| \angle pc' \leq (1 - 2\sqrt{\varepsilon_2}) O(\varepsilon + \sqrt{\delta}) \rho_x.$$

Now we can bound the distance $\|c - p^+\|$ if we have a bound on $\|c' - p^+\|$. We will apply Lemma 6 to the ball $B'' = B_{c',\|p-c'\|}$ to bound $\|c' - p^+\|$. Since $m_x \in M_\alpha$ there are two points x and x' in Σ so that $\angle x m_x x' \geq \alpha$. Take z in Lemma 6 as the point x or x' which makes the angle $\angle z m_x p$ at least $\alpha/2$.

With this set up we show that β and ε' in Lemma 6 are $1 - O(\sqrt{\varepsilon} + \sqrt{\delta})$ and $O(\varepsilon + \sqrt{\delta})$ respectively. Since the radius of B'' is $r \geq (1 - 2\sqrt{\varepsilon_2}) \rho_x = (1 - 2\sqrt{\varepsilon_2}) \rho_z$, the claim for β follows.

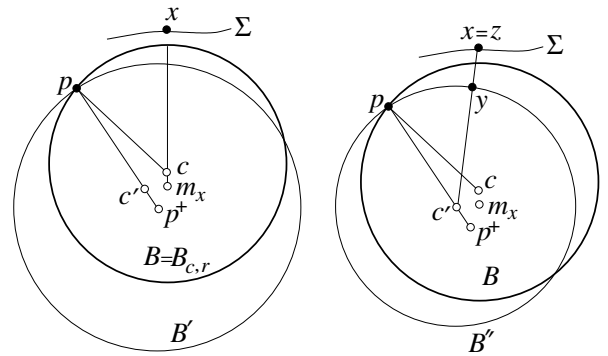


Figure 7: Illustration for Theorem 2. The ball $B_{c,r}$ is deformed to the Delaunay ball $B' = B_{p^+,r'}$. The ball $B'' = B_{c',\|p-c'\|}$ on the right is a shrunk version of B' .

For ε' , consider the point y where the ray $\vec{c'z}$ meets the boundary of B'' , refer to Figure 7. We have $\|c' - m_x\| \leq \|c - m_x\| + \|c - c'\| = O(\sqrt{\varepsilon} + \sqrt{\delta}) \rho_x$ and hence

$$\begin{aligned}
\|y - z\| &= \|c' - z\| - \|c' - y\| \\
&\leq \|m_x - z\| + \|c' - m_x\| - \|c' - y\| \\
&\leq \rho_z + O(\sqrt{\varepsilon} + \sqrt{\delta})\rho_z - (1 - 2\sqrt{\varepsilon_2})\rho_z \\
&= O(\sqrt{\varepsilon} + \sqrt{\delta})\rho_z.
\end{aligned}$$

So, we can apply Lemma 6 with $\varepsilon' = O(\sqrt{\varepsilon} + \sqrt{\delta})$, and $\beta = 1 - O(\sqrt{\varepsilon} + \sqrt{\delta})$. Observe that, since the points c' and m_x are nearby, the angle $\angle pc'y$ is almost equal to $\angle zm_xp$. So, we can safely assume $\angle pc'y \geq \frac{\alpha}{4}$. With $\alpha = \varepsilon^{\frac{1}{4}} + \delta^{\frac{1}{4}}$, Lemma 6 gives

$$\begin{aligned}
\|p^+ - c'\| &= (O(\varepsilon^{\frac{1}{2}} + \delta^{\frac{1}{2}})/\Omega(\varepsilon^{\frac{1}{4}} + \delta^{\frac{1}{4}}))\rho_z \\
&= O(\varepsilon^{\frac{1}{4}} + \delta^{\frac{1}{4}})\rho_z.
\end{aligned}$$

The claim of the theorem follows as

$$\begin{aligned}
\|p^+ - m_x\| &\leq \|p^+ - c'\| + \|c' - m_x\| \\
&= O(\varepsilon^{\frac{1}{4}} + \delta^{\frac{1}{4}})\rho_x + O(\varepsilon^{\frac{1}{2}} + \delta^{\frac{1}{2}})\rho_x \\
&= O(\varepsilon^{\frac{1}{4}} + \delta^{\frac{1}{4}})\rho_x.
\end{aligned}$$

□

For each point $x \in \Sigma$ where $m_x \in M_\alpha$ the previous theorem guarantees the existence of a sample point p whose pole approximates m_x . Actually, the proof technique can also be used to show that any Delaunay ball with radius almost as big as ρ_x and incident to a sample point close to x has its center close to m_x .

Theorem 3. *Let $x \in \Sigma$ be a point so that $m_x \in M_\alpha$ for $\alpha = \varepsilon^{\frac{1}{4}} + \delta^{\frac{1}{4}}$. Then for any point $p \in P$ within $\varepsilon_3\rho_x$ distance of x and with an incident Delaunay ball of radius at least $(1 - O(\sqrt{\varepsilon} + \sqrt{\delta}))\rho_x$, the pole p^+ lies within $O(\varepsilon^{\frac{1}{8}} + \delta^{\frac{1}{8}})\rho_x$ distance from m_x .*

sketch. Notice that if $\mathbf{n}_{\tilde{p}}$ and \mathbf{n}_x make small angle, we will be done. Then, we have two segments pp^+ and xm_x almost parallel where p and x are close. Also, these segments can be shown to be of almost same lengths by the given condition and a proof similar to that of Theorem 2. This would imply m_x and p^+ are close.

Observe that we cannot assert that $\angle \mathbf{n}_{\tilde{p}}, \mathbf{n}_x$ is small directly from the normal variation lemma in Amenta and Bern [2] as the distance among them is at most $\varepsilon_3\rho_x$ by Lemma 4 (notice ρ_x vs. $f(x)$). Since p and x are at most $\varepsilon_3\rho_x$ apart and the distance of p^+ to p and hence to x is $\Omega(\rho_x)$, $\angle pp^+x = O(\varepsilon_3)$. By Corollary 5, it can be shown that p^+x makes $O(\sqrt{\varepsilon_3})$ angle with \mathbf{n}_x . Therefore, pp^+ makes $O(\sqrt{\varepsilon_3})$ angle with \mathbf{n}_x . It is easy to show that ρ_x is at least $\Omega(f(\tilde{p}))$. So, the angle between pp^+ and $\mathbf{n}_{\tilde{p}}$ is $O(\sqrt{\varepsilon_3}) = O(\varepsilon^{\frac{1}{8}} + \delta^{\frac{1}{8}})$. One can deduce that $\|p^+ - m_x\|$ has the claimed bound with $\angle \mathbf{n}_{\tilde{p}}, \mathbf{n}_x = O(\sqrt{\varepsilon_3})$. □

5.2 Algorithm

Theorem 2 and Theorem 3 suggest the following algorithm for feature estimation at any point $x \in \Sigma$ where $m_x \in M_{\varepsilon^{\frac{1}{4}} + \delta^{\frac{1}{4}}}$. Theorem 2 says that x has a sample point p within a neighborhood of $\varepsilon_3\rho_x$ whose pole p^+ approximates m_x . Also, Theorem 3 says that *all* sample points within $\varepsilon_3\rho_x$ neighborhood of x with a large enough Delaunay ball have their poles approximate m_x . Therefore, if we take the pole of a sample point q whose distance to q is largest among all sample points within a neighborhood of x , we will get an approximation of m_x .

We search the neighborhood of x by taking k nearest neighbors of a sample point s close to x . If we assume that P is a $(\varepsilon, \delta, \kappa)$ -sample for some $\kappa > 0$, κ -nearest neighbors cannot be arbitrarily close to x . Notice that if we do not prevent oversampling by the third condition of noisy sampling, we cannot make this assertion. In the algorithm, we simply allow an user supplied parameter k to search the k nearest neighbors. Since we want to cover all points of Σ , we simply take all points of P and carry out the following computations.

For each point $p \in P$ we select k -nearest neighbors for a suitable k . Let N_p be this set of neighbors. First, for each $q \in N_p$, we determine the Voronoi vertex v_q in V_q which is furthest from q . This is one of the poles of q . Let $\ell_1(p) = \|v_q - q\|$. Select the point $p_1 \in N_p$ so that $\ell_1(p_1)$ is maximum among all points in N_p . By Theorem 2 and Theorem 3, v_{p_1} approximates a medial axis point m_x if $x \in M_{\varepsilon^{\frac{1}{4}} + \delta^{\frac{1}{4}}}$. However, we do not know if m_x is an inner medial axis point or an outer one. Without loss of generality assume that m_x is an inner medial axis point. To approximate the outer medial axis point for x , we determine the Voronoi vertex u_q in V_q for each $q \in N_p$ so that $q\vec{u}_q$ makes more than $\frac{\pi}{2}$ angle with $p_1\vec{v}_{p_1}$. Let $\ell_2(q) = \|u_q - q\|$. Then, we select the point $p_2 \in N_p$ so that $\ell_2(p_2)$ is maximum among all points in N_p . Again, appealing to Theorem 2 and Theorem 3 for outer medial axis, we can assert that u_{p_2} approximates a medial axis point for x .

APPROXIMATEFEATURE(P, k)

```

Compute Del  $P$ ;  $L := \phi$ ;
for each  $p \in P$  compute  $k$  nearest neighbors  $N_p$ ;
  compute  $p_1 \in N_p$  whose distance to
  its pole  $v_{p_1}$  is maximum
  among all points in  $N_p$ ;
  compute  $p_2 \in N_p$  with a pole  $v_{p_2}$  so that
   $\angle p_2\vec{v}_{p_2}, p_1\vec{v}_{p_1} \geq \frac{\pi}{2}$  and  $\|p_2 - v_{p_2}\|$ 
  is maximum among  $N_p$ ;
   $L := L \cup \{v_{p_1}, v_{p_2}\}$ ;
endfor
for each  $p \in P$  compute the distance of  $p$  to  $L$ .

```

As we have observed already, a subset of the medial

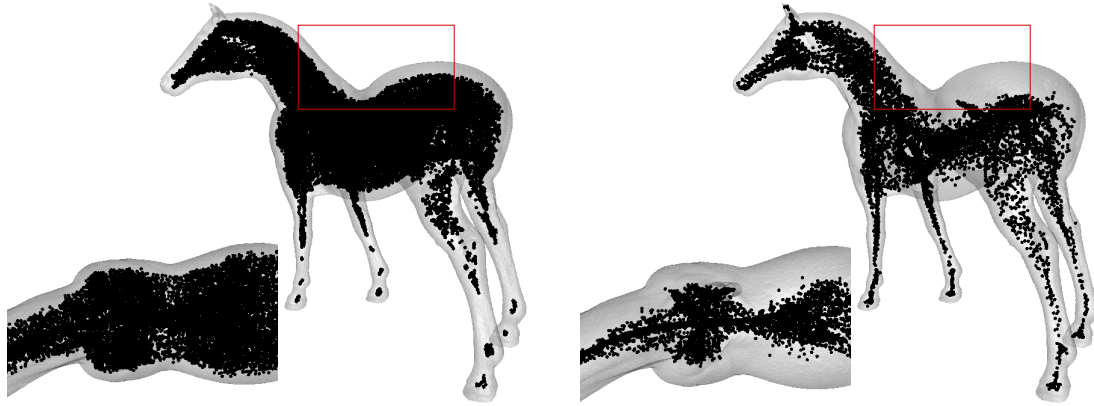


Figure 8: Left: Medial axis approximated by centers of big Delaunay balls for a noisy HORSE. For a chosen threshold, some parts of the legs do not have medial axis approximated though still many centers lie near the surface. Right: Medial axis well approximated by the poles as computed by APPROXIMATEFEATURE.

axis is not approximated by the poles. These are exactly the points on the medial axis which have a small medial angle. This type of exclusions are also present in earlier medial axis approximation results [4, 6, 7]. The implication of this exclusion is that features cannot be properly estimated for points whose closest point on the medial axis resides in the excluded part. However, if the sampling is sufficiently dense, the excluded part is indeed small in most cases. Figure 8 shows the result of feature approximations for a model in three dimensions.

References

- [1] M. Alexa, J. Behr, D. Cohen-Or, S. Fleishman, D. Levin and C. Silva. Point set surfaces. *Proc. IEEE Visualization* (2001), 21–28.
- [2] N. Amenta and M. Bern. Surface reconstruction by Voronoi filtering. *Discr. Comput. Geom.* **22** (1999), 481–504.
- [3] N. Amenta, M. Bern and D. Eppstein. The crust and the β -skeleton: combinatorial curve reconstruction. *Graphical Models and Image Processing*, **60** (1998), 125–135.
- [4] N. Amenta, S. Choi and R. K. Kolluri. The power crust, union of balls, and the medial axis transform. *Comput. Geom.: Theory Applications* **19** (2001), 127–153.
- [5] D. Attali and A. Montanvert. Modeling noise for a better simplification of skeletons. *Proc. Internat. Conf. Image Process.* **3**, 13–16, 1996.
- [6] J. D. Boissonnat and F. Cazals. Natural neighbor coordinates of points on a surface. *Comput. Geom. Theory Applications* (2001), 87–120.
- [7] F. Chazal and A. Lieutier. Stability and homotopy of a subset of the medial axis. *Proc. ACM Sympos. Solid Modeling and Applications* (2004), 243–248.
- [8] T. K. Dey and S. Goswami. Provable surface reconstruction from noisy samples. *Proc. 20th Annu. Sympos. Comput. Geom.* (2004), 330–339.
- [9] T. K. Dey and J. Sun. Adaptive MLS surfaces for reconstruction with guarantees. *Proc. Eurographics Sympos. Geom. Processing* (2005), 43–52.
- [10] T. K. Dey and W. Zhao. Approximating the medial axis from the Voronoi diagram with a convergence guarantee. *Algorithmica* **38** (2003), 179–200.
- [11] R. Kolluri. Provably good moving least squares. *Proc. ACM-SIAM Sympos. Discrete Algorithms* (2005), 1008–1017.
- [12] B. Mederos, N. Amenta, L. Velho and H. de Figueiredo. Surface reconstruction from noisy point clouds. *Proc. Eurographics Sympos. Geom. Processing* (2005), 53–62.
- [13] N. Mitra, J. Nguyen and L. Guibas. Estimating surface normals in noisy point cloud data. *Internat. J. Comput. Geom. & Applications* (2004).
- [14] M. Pauly, R. Keiser, L. Kobbelt and M. Gross. Shape modeling with point-sampled geometry. *Proc. ACM SIGGRAPH 2003*, 641–650.
- [15] www.cse.ohio-state.edu/~tamaldey/normfet.html